Published in final edited form as:
J Phys Chem C Nanomater Interfaces. 2013 May 9; 117(18): . doi:10.1021/jp3091667.

Luminescent Properties of Eu(III) Chelates on Metal Nanorods

Jian Zhang[†,*], **Yi Fu**[†], **Krishanu Ray**, **Yuan Wang**[‡], and **Joseph. R. Lakowicz**[†]

[†]Center for Fluorescence Spectroscopy, University of Maryland School of Medicine, Department of Biochemistry and Molecular Biology, 725 West Lombard Street, Baltimore, Maryland 21201, United States

[‡]College of Chemistry and Molecular Engineering, Peking University, Beijing National Laboratory for Molecular Sciences, Beijing 100871, P. R. China

Abstract

In this article, we report the change of optical properties for europium chelates on silver nanorods by near-field interactions. The silver rods were fabricated in a seed-growth method followed by depositing thin layers of silica on the surfaces. The europium chelates were physically absorbed in the silica layers on the silver rods. The silver rods were observed to exhibit two plasmon absorption bands from longitudinal and transverse directions, respectively, centered at 394 and 675 nm, close to absorption and emission bands from the Eu(III) chelates. As a result, the immobilized Eu(III) chelates on the silver rods should have strong interactions with the silver nanorods and lead to greatly improved optical properties. The Eu–Ag rod complexes were observed to have enhanced emission intensity up to 240-fold in comparison with the Eu(III) chelates in the metal-free silica templates. This enhancement is much larger than the value for the Eu(III) chelates on the gold rods or silver spheres indicating the presence of stronger interactions for the Eu(III) chelates with the silver rods. The interactions of Eu(III) chelates with the silver rods were also proven by extremely reduced lifetime. Moreover, the Eu–Ag rod complexes exhibited a polarized emission, which was also due to strong interactions of the Eu(III) chelates with the silver rods. All of these features may promise that the Eu(III)–Ag rod complexes have great potential for use as fluorescence imaging agents in biological assays.

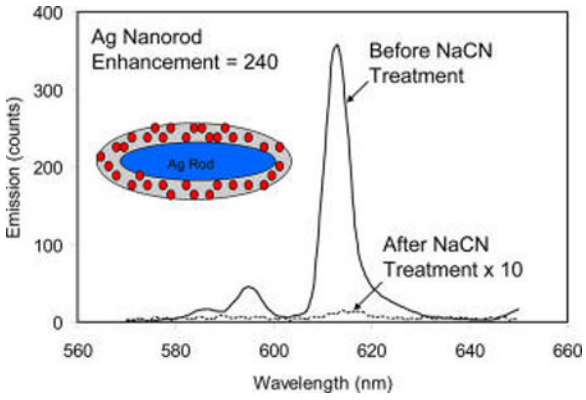

[*]**Corresponding Author**, jianzhang@umaryland.edu; tel: 410-706-7500; fax: 410-706-8409.

The authors declare no competing financial interest.

INTRODUCTION

It is known that a lanthanide emits luminescence with a large Stokes shift, narrow emission band, and long lifetime, so the use of lanthanide dyes may offer an opportunity to create a sensitive time-resolved bioassay or cell imaging with a low luminescence background.[1,2] However, the emission from the lanthanide may involve an electron transition in its 4f orbits, which is basically forbidden, so in comparison with a conventional organic fluorophore the lanthanide dye often has an extremely low absorbance coefficient and a very slow emissive rate.[3] Consequently, the lanthanide dye often displays a low quantum yield and brightness, and a lanthanide-based fluorescence bioassay often results in a low detection sensitivity. In addition, the lanthanide dye has an extremely long decay time up to milliseconds, which may often bring up a low photon count rate in the emission and result in low emission intensity. Therefore, the single molecule detection (SMD) of the lanthanide dye is not reported to date.[4]

With advances in coordination chemistry, new lanthanide chelates have been developed with significantly improved optical properties.[1,2] Basically, these lanthanide chelates are created by coordinating chromophores with lanthanide ions, in which the chromophores can act as antennas or sensitizers to absorb photons and subsequently transfer the photons to the lanthanide centers for increasing their emission rates and efficiencies. In comparison with the lanthanide ions, these lanthanide chelates have significantly increased optical properties including brightness and quantum yields. Because of absorption from the ligands, the lanthanide chelates often exhibit a broader excitation range leading to a significant shift of maximal excitation wavelength to the red region.[5] Hence, it is believed that the formation of lanthanide chelates may overcome some inherent weakness of lanthanide dyes especially on the absorption cross-section and excitation wavelength. However, it is also noticed that the decay rate of the lanthanide center in the chelate is not really increased with the coordination.[6] Therefore, there is a basic research need to develop a strategy that can increase the radiative rate of the lanthanide chelate and furthermore increase the cyclic number for the excitation/emission of Eu(III) chelate in a period of time and the photon count rate in the measurement.

The near-field interaction approach is considered to enable use for such a purpose. Fundamentally, as induced by an incident light, the metal nanoparticle of subwavelength size can create a local electric field around it.[7,8] When a fluorophore is put in the local field within a near-field range from the metal nanoparticle, the coupling interaction between the fluorophore and metal nanoparticle can increase the radiative rate of the fluorophore and furthermore enhance the emission intensity of the fluorophore up to 10- to 10^3-fold.[9–12] Increased radiative rate of the fluorophore may also bring a decrease in the lifetime.[9] Thus, the metal-enhanced fluorescence (MEF) by the near-field interaction effect is often accompanied with a decrease of lifetime for a fluorophore. In this study, the near-field interaction approach was employed to improve the optical properties of lanthanide chelates. Typically, the lanthanide chelates were immobilized on the metal nanoparticles within a near-field range to initiate the coupling interactions. The feasibility of this approach has been demonstrated by one of our earlier reports in which the lanthanide chelates were localized in the cores of silver shells and the emission could be greatly enhanced due the near-field interactions.[13] More work is needed to optimize the conditions for achieving maximally enhanced luminescence.[14–16] Importantly, the silver shells in the earlier report were found to exhibit only one plasmon band that is localized between the absorption and emission bands of Eu(III) chelate.[13] Even though the interactions in the near-field range cannot be completely reflected by the observations on the far-field spectra,[9] we still believe that it is important to achieve the maximally spectral overlapping from the fluorophores and metal nanoparticles to achieve the efficient near-field interaction between them. Of course,

the couplings between the lanthanide chelates and metal shells were considered to be insufficient.[9] Actually, it is almost impossible to fabricate a metal shell, which displays only a single plasmon band enabling a sufficient coupling with a lanthanide chelate, which has a very large Stokes shift at both its excitation and emission bands. Therefore, new metal substrates are needed.

Metal nanorods have been widely reported as new nanoparticle substrates.[17,18] We were interested in the metal rods and intended to use them as the substrates to couple with the lanthanide chelates because the metal rods can display two separated plasmon bands from the longitudinal and transverse directions, respectively, and the band maxima can be tuned with the aspect ratio of metal rods.[17,18] Particularly, we have research interest in silver nanorods because the silver rods can display two plasmon bands close to the absorption and emission maxima from the Eu(III) chelates. In this study, the silver rods were fabricated in a chemical method followed by depositing the silica layers on the surfaces. The Eu(III) chelates were physically absorbed in the silica layers on the silver rods within the near-field range from the metal surfaces. Optical properties from the Eu(III) chelates on the silver rods were determined on an ensemble fluorescence spectrophotometer with the time-gated conditions. Compared with the emission properties of Eu(III) chelates in the metal-free silica templates, the influences from the silver rods to the emission of Eu(III) chelates could be explored. The gold rods and silver spheres were also fabricated and immobilized with the Eu(III) chelates in the same strategy. The optical properties from the Eu–Au rod and Eu–Ag sphere complexes were determined as controls of the properties on the silver rods.

Polarized emission is regarded as an important feature for a fluorophore in biological and medical applications.[4,19,20] Because the emission from a lanthanide chelate arises from a high-spin-high-spin transition,[21,22] which involves multiple transition dipole moments that are energetically degenerated, it is generally unpolarized. Moreover, an extremely long lifetime may offer the lanthanide chelate enough time to make a rotational motion during its excited state so the emission is mostly unpolarized. Hence, there is a particular research interest to find a strategy that can be used to initiate a polarized emission from the lanthanide chelate. So far, some reports appear,[23–25] in which the lanthanide chelates were mostly immobilized in aligned matrixes such as liquid crystals and stretched polymer films, or the single crystals of lanthanide complexes were used to restrict the motions and realize the polarized emission. However, neither of these approaches is inappropriate for the uses of lanthanide-based assays. A recent publication shows us another alternation,[26a] in which the near-field interaction on the metal nanoparticle can alter the transition moment of a fluorophore and finally initiate a polarized emission from the fluorophore. Therefore, aside from enhanced luminescence, we expected that the interactions for the Eu(III) chelates on the silver rods could initiate the polarized emission from the lanthanide chelates.

EXPERIMENTAL SECTION

All reagents and spectroscopic grade solvents were used as received from Fisher or Sigma/ Aldrich. Tris-(dibenzoylmethanate)mono(5-amino-1,10-phenanthroline) europium chelates were commercially available from Sigma/ Aldrich. Nanopure water (>18.0 $M\Omega \bullet cm^{-1}$) purified on a Millipore Milli-Q gradient system was used in all experiments.

Preparation of Metal Nanorods

In a modified seed growth method, the silver nanorods were fabricated in aqueous solutions with a defined aspect ratio.[26–28] In brief, small silver nanoparticles were first generated as a seed solution to initiate the growth of silver rods. Typically, 20 mL aqueous solution with 0.25 mM $AgNO_3$ and 0.50 mM sodium citrate was added by 1 mL of ice-cold 0.1 M $NaBH_4$ solution with rigorous stirring. The color of solution was turned to yellow representing the

formation of small silver nanoparticles, which had an average diameter of 4 nm. For the silver rod fabrication, 10 mL of aqueous solution with 0.25 mM $AgNO_3$, 80 mM cetryltrimethylammoium bromide (CTAB), and 0.5 mM ascorbic acid were added to a 30 μ*L* seed solution. The mixing solution was continuously stirred for 30 min. The color of the solution changed from yellow to green representing the formation of silver rods. The formed silver rods were collected by centrifugations followed by dispersing in 1 mL of mixing solvent of water/ethanol (v/v = 1) for depositing the silica layers on the external surfaces.

The gold nanorods and silver spheres were also fabricated and used as controls of silver rods. The gold rods were fabricated in the same strategy as the silver rods. In the strategy of our earlier report, the silver spheres were fabricated to have an average diameter of 40 nm.[15] Like the silver rods, the gold rods and silver nanospheres were respectively redispersed in 1 mL of mixing solvent of water/ethanol (v/v = 1) for depositing the silica layers on the external surfaces.

Depositing Silica Layers on Metal Nanoparticles

In a modified Stöber method, thin silica layers were deposited on the metal nanoparticles including silver rods, gold rods, and silver spheres for immobilizing the europium chelates.[29,30] Typically, 1 mL of metal nanoparticle solution was added by 1 mL of water/ethanol (v/v = 1) solution containing 1×10^{-3} M tetraethyl orthoorthosilicate. Subsequently, 10 μ*L* of 30% ammonia solution was added dropwise under vigorous stirring. The solution was stirred overnight at room temperature to form the silica layers on the metal nanoparticles. The suspension solution was removed by centrifugation, and the residual solid was dispersed in 1 mL of a mixing solvent of *N*,*N*-dimethylformamide (DMF)/alcohol (v/v = 1/1) for immobilizing the europium chelates.

Immobilizing Eu(III) Chelates on Metal Nanoparticles

Tris(dibenzoylmethanate)mono(5-amino-1,10-phenanthroline) europium chelates were immobilized into the silica layers on the metal nanoparticles via physical absorptions.[13] The Eu(III) chelates (1×10^{-5} M) were codissolved in a mixing solution of DMF/alcohol (v/v = 1/1) containing the silica-treated metal nanoparticles (1×10^{-8} M). The solution was stirred for 12 h at room temperature, and the suspension was removed by centrifugation. The residual solid was subsequently washed with DMF, ethanol, and water. The collected metal nanoparticles were dispersed in water for the ensemble spectral measurements.

Ensemble Spectral and Anisotropy Measurements

Absorption spectra were conducted on a Hewlett-Packard 8453 spectrophotometer. Ensemble fluorescence spectra were recorded with a Cary Eclipse Fluorescence Spectrophotometer. Because of a slow decay time of Eu(III) chelate, a time-gated technique was used to collect the emission from the lanthanide, in which the gate pulse width was 0.5 ms and the delay time was 0.1 ms. All Eu(III) chelate-associated samples were excited at 380 nm for their emission spectral collections. In the current measurements, the polarized emission of Eu(III) chelate-associated samples were determined with two orthogonal polarizations, one parallel and one perpendicular to the excitation polarization vector.[4] The emission anisotropies of Eu(III) chelate-associated samples were determined in the single-channel method under the same time-gate conditions.[4] In general, the emission anisotropies can be expressed as,[4]

$$r = \frac{I_{\parallel}/I_{\perp} - 1}{I_{\parallel}/I_{\perp} + 2} \quad (1)$$

in which $I_{\|}$ is the intensity of the emitted light when the emission polarizer is oriented parallel to the direction of the excitation polarization, whereas $I_{\perp}$ is the intensity of emitted light when the emission polarizer is perpendicular to the direction of the polarized excitation. The monochromator will have different transmission efficiency for vertically and horizontally polarized light, and as a result the excitation intensity can change when the excitation polarizer is rotated. Thus, in the single-channel method measurements, the emission intensities ($I_{\|}$ and $I_{\perp}$) have been normalized to correct for the polarization sensitivity of the detection pathway in eq 2.

$$I_{\|}/I_{\perp}=\frac{I_{\mathrm{VV}}I_{\mathrm{HH}}}{I_{\mathrm{VH}}I_{\mathrm{HV}}} \quad (2)$$

I_{VV}, I_{HH}, I_{VH}, and I_{HV} are the emission intensities measured on the different directions for two polarizers installed on the excitation and emission sides. Angle-dependent luminescence from the Eu–meal complexes were measured by adjusting the angle between the two polarizers of excitation and emission sides and corrected using the emission from the free Eu(III) chelates in solution that was considered to be completely unpolarized.

TEM Image

For the TEM measurements, the nanoparticle samples were diluted to nanomolar concentrations followed by casting onto the copper grids (200 mesh) with standard carbon-coated Formvar films (200–300 Å). The samples were dried in air. TEM images were taken with a side-entry Philips electron microscope at 120 keV. The distributions of nanoparticle sizes were analyzed with Scion Image Beta Release 2 on the base on at least 200 images.

RESULTS AND DISCUSSION

In this study, the silver nanorods were fabricated in a modified seed growth method.[26–28] The achieved silver rods could be distinctly outlined by TEM images (part a of Figure 1) showing an average length of 80 nm and width of 18 nm. As a control, the gold rods were also fabricated in the similar strategy and outlined by TEM image showing an average length of 60 nm and width of 20 nm (part b of Figure 1). The aspect ratios of metal rods hence were estimated to be ca. 5 for the silver and ca. 3 for the gold. These metal rods were stabilized by cetryltrimethylammoium bromide (CTAB) on the surfaces. As expected, the metal rods exhibited distinct two plasmon absorption bands from the longitudinal and transverse directions, respectively, in aqueous solution (Figure 2), on which the bands from the silver rods were centered at 394 and 675 nm and the bands from the gold rods were centered at 536 and 982 nm. Tris(dibenzoylmethanate)mono(5-amino-1,10-phenanthroline) europium chelate was employed to immobilize on the metal rods for exploring the near-field interactions. It was observed that this Eu(III) chelate exhibited an absorption band and an emission band centered at 353 and 614 nm (Figure 3), respectively, close to the plasmon bands from the silver rods. Thus, there were sufficient spectral couplings between the Eu(III) chelates and silver rods at both the excitation and emission processes, and as a result the Eu(III) chelates in the near-field range from the metal rods were expected to have strong interactions with the silver rods leading to greatly improved optical properties. As the control of silver rods, the gold rods were observed to display the plasmon bands significantly shifting to the red region and, thus, could not sufficiently couple with the absorption and emission bands from the Eu(III) chelates, and the emission from the Eu(III) chelates on the gold rods should be less enhanced.

The Eu(III) chelates were immobilized in the silica layers on the metal rods. Because the Eu(III) chelates were required to localize in the near-field range, the silica layers on the metal rods were thin. Typically, the metal rods were deposited by thin silica layers through a

hydrolysis reaction of tetraethyl orthosilicate.[29,30] By the ratio of orthosilicate monomer over the metal rod in the reaction solution, the silica layer on the metal rod was controlled to be ca. 5 nm thick. The silane-treated metal rods were dispersed in a mixed solvent of DMF/alcohol containing Eu(III) chelates to absorb the Eu(III) chelates from solution by physical interactions . The Eu–metal rod complexes were recovered by configuration and dispersed in water for the spectral measurements. It was difficult to outline the silica layers from the metal rods on the TEM images because of their thin thickness. But they could be identified by the emission spectral measurements. For the silane-treated metal rods, there was significant luminescence detectable after absorbing the Eu(III) chelates, whereas for the untreated metal rods there was no luminescence after absorbing the Eu(III) chelates supporting that there were the silica layers formed on the metal rods after the silane-treatments.

In the absorption process of Eu(III) chelates into the silane-treated metal rods, the Eu(III) chelates and silane-treated metal rods were codissolved at a molar ratio of 1000/1 in solution. According to the concentration change of Eu(III) chelate in solution prior to and after the absorption treatment, the consuming amount of Eu(III) chelate in solution was estimated, and thus, the amount of Eu(III) chelate absorbed on the metal rods was inferred. As a result, the number of Eu(III) chelate on one metal nanoparticle could be approximately estimated. This number was estimated to be ca. 650 on the silver rod and ca. 560 on the gold rod. The loading number of Eu(III) chelate on the silver rod corresponds to approximately 5 M, which is extremely high for most organic dyes in the solid matrixes. But for the Eu(III) chelates, there was no serious quenching to occur among them because of a large Stokes shift.[1,2] Actually, most lanthanide-based nanoparticles are fabricated with high loading number of chelate for maximally increasing their brightness. The loading number of Eu(III) on the metal rod hence was considered to be acceptable in this study.

The Eu(III)–Ag rod complexes were observed to display two plasmon bands and the band maxima remained almost unchanged from those from the CTAB-coated silver rods, indicating the silver rods were chemically stable in the surfaces reactions. The Eu(III) chelates were immobilized on the metal rods but the immobilized Eu(III) chelate so the metal rods could not be determined by the absorption spectrum because of strong interference from the plasmon bands from the metal rods. Thus, the emission spectrum was used to determine the Eu(III) chelates on the silver rods. It was shown that upon excitation at 380 nm the Eu(III)–Ag rod complexes displayed an emission band centered at 610 nm (Figure 4), a 4 nm shift to blue in comparison with the free Eu(III) chelates. The emission band from the Eu(III)–Ag rod complexes was also significantly broadened, which was primarily due to the restriction of the movements of Eu(III) chelates after they were immobilized in the solid templates as well as the structural heterogeneity of Eu(III) chelates in the nearby environments.[31] In fact, it has been widely reported that the emission band becomes broadened with the immobilization of fluorophores into the solid substrates in comparison with that in solution. These fluorophores include not only lanthanide chelates but also many other organic fluorophores. The breakdown of beta-diketonate by the acidic conditions in the silica is also considered as a possible reason causing such broadness. But because there is no significant change in the emission spectrum except the broadness with the immobilization of Eu(III) chelates in the silica, we suggest that the restriction of movement for the immobilized fluorophore in the solid substrate and influence from the heterogeneous surrounding is still the primary reason causing such a change in the band broadness.

The near-field interactions of Eu(III) chelates with the silver rods were supposed to explore by the optical property change for the Eu(III) chelates in the silica templates in the presence or absence of silver rods. In brief, the silver rods could be removed by adding several drops

of 0.1 N NaCN solution into the Eu–Ag rod complex solution. With the dissolution of metal rods, the metal-free Eu(III) chelate-contained silica templates were consequently released.[32] Apparently, it was observed that the color of plasmon from the metal rods disappeared progressively, and, simultaneously, the emission intensity from the Eu(III) chelates was decreased due to the loss of near-field interaction. Finally, the solution became completely colorless and the emission from the Eu(III) chelates was reduced to a minimum (Figure 4). However, the wavelength and broadness of the emission band from the Eu(III) chelates were not significantly altered with the dissolution of metal rods indicating that the Eu(III) chelates were still immobilized in the metal-free silica templates. To test the possible influence from adding NaCN to luminescence from the Eu(III) chelates in the silica templates, the emission from the Eu–silica templates were subsequently monitored by addition of NaCN aqueous solution. It was shown that the emission remained almost unchanged indicating that the emission from the Eu(III) chelates in the silica templates was not significantly influenced by NaCN in solution.

The emission intensity from the Eu–Ag rod complexes was reduced with the dissolution of metal rods representing that the emission from the Eu(III) chelates was indeed enhanced on the metal rods due to the near-field interactions. The enhancement efficiency was estimated by the ratio of the emission intensity from the Eu–Ag rod complexes prior to the NaCN treatment over the intensity after the treatment. The value was estimated to be 240-fold (part a of Figure 5). As the control, the Eu–Au rod complexes were also treated in the same strategy and the enhancement efficiency was estimated to be 14-fold. The enhancement for the Eu(III) chelates on the gold rods was much smaller than that on the Ag rods representing that the Eu(III) chelates had stronger interactions with the silver rods as expected early. Basically, the silver rods have their transverse and longitudinal plasmon bands close to the absorption and emission bands of Eu(III) chelates, which might lead to stronger interactions on the silver rods.

For a fluorophore, the near-field interaction at the emission process can increase its radiative rate and furthermore enhance its luminescence.[9] However, the increased radiative rate of a fluorophore can be reflected by its decreased lifetime. The lifetimes from the Eu(III) chelates on the metal rods were collected by the time-gated method in this study. The decay curves from the Eu–Ag rod complexes and metal-free silica templates were presented in Figure 6 showing different decay rates. The curves were analyzed in terms of a two-exponential model, and the lifetime data were presented in average values (part b of Figure 5). It is shown that the free Eu(III) chelates in solution have a lifetime of 75 μs (not shown in figure). After immobilizing the Eu(III) chelates in the silica templates, the lifetime was increased to 0.5 ms, which was primarily due to the restriction of movements of Eu(III) chelates in the solid templates as discussed earlier.[33] On the silver rods, the lifetime of Eu(III) chelates was dramatically reduced to be less than 10 μs. We suppose that it was primarily because of strong near-field interactions of Eu(III) chelates with the silver rods. As the control, the lifetime of Eu–Au rod complexes was also measured and estimated to be 70 μs. This value is shorter than the lifetime on the metal-free silica templates but much longer than the lifetime on the silver rods implying that the Eu(III) chelates had interactions with the gold rods but the interactions were much weaker than those with the silver rods. This result is approximately consistent with the observation achieved from the emission intensity for the Eu(III) chelates on the metal rods.

For a near-field interaction, a fluorophore is known to interact with a metal nanoparticle at either the excitation or emission process of the fluorophore. But the changed lifetime of the fluorophore by the metal nanoparticle can only reflect the interaction at the emission process.[9] In this case, the lifetime of Eu(III) chelates on the silver rods was reduced by 50-fold (Figure 6). But the emission intensity was enhanced by 240-fold. The enhancement fold

on the emission intensity is significantly larger than the decrease fold on the lifetime. Thus, it is suggested that the enhanced luminescence for the Eu(III) chelates on the silver rods should arise at least partially from the interactions at the excitation process. A sufficient spectral coupling between the absorption band from the Eu(III) chelates and the transverse plasmon band from the silver rods can support this speculation. In contrast, the enhanced luminescence from the Eu(III) chelates on the gold rods should arise almost completely from the emission process rather the excitation process due to the lack of sufficient spectral coupling at the excitation region.

It is important to understand how the near-field interaction on the metal rod can influence how the emission lines form the europium center for the chelate. It is known that the Eu(III) center in the chelates can accept the energy from all ^{5}D orbits.[1,2] However, although the Eu(III) centers in the chelates can emit a luminescence from the $^5D_1$ level, the main transitions may originate from the $^5D_0$ level that correspond to the main emission line at 614 nm (Figure 3). With the immobilization of Eu(III) chelates in the silica layers and interactions with the metal nanoparticles, the emission bands from the Eu(III) chelates were significantly broadened. As a result, the detail lines from the emission bands could not be distinguishable. Thus, it is difficult to understand the influence from the near-field interactions on the transitions of Eu(III) centers in the chelates. But because of sufficient spectral overlapping of absorption and emission bands from the Eu(III) chelates with the plasmon bands from the silver rods, we expect that in this case the Eu(III) chelates can interact efficiently with the silver rods at all of their energy levels.

To demonstrate the role of silver rods in the near-field interactions, the 40 nm silver spheres were also fabricated and the 5 nm thick silica layers were deposited on the silver spheres for immobilizing the Eu(III) chelates. Different from the silver rods, the silver spheres exhibited only one plasmon band centered at 460 nm[15,16] localized between the bands of absorption and emission from the Eu(III) chelates. As a result, the spectral coupling on the silver spheres should be not sufficient as it is on the silver rods. Thus, it is no surprise that the Eu(III) chelates expressed weaker interactions with the silver spheres relative to the Eu(III) chelates on the silver rods. The enhancement efficiency on the silver spheres was determined to be 80-fold lower than that on the silver rods, and the lifetime was reduced to 30 μs, longer than the lifetime on the silver rods. Both data showed that the interactions of Eu(III) chelates on the silver spheres were weaker than those on the silver rods. According to reports, the silver ions that were dissolved from the metal rods were supposed to interact with the ligands from the chelates, which could probably enhance the emission from the Eu(III) chelates.[13] But because most silver on the nanoparticles were presented as a noble metal rather than as ions, it is believed that the influence from the silver ions should be much less in comparison with the near-field interaction effect.

It is also known that the near-field interaction for a fluorophore on a metal nanoparticle is distance-dependent.[9] When the fluorophore is localized too close to the metal nanoparticle, the absorption effect is a domain factor and the emission from the fluorophore is quenched, whereas with an increase of distance from the fluorophore to the metal nanoparticle but still within the near-field range, the scattering effect becomes a domain effect and the emission from the fluorophore becomes enhanced.[9,14] Plenty of studies have reported on this topic. In this work, we deposited 5 nm thick silica layers on the metal rods and the Eu(III) chelates were physically absorbed in the silica to explore the near-field interactions. We believe that all Eu(III) chelates should be localized within the near-field range from the metal rod. The emission from a portion of Eu(III) chelates proximate to the metal surfaces would be quenched but the emission from most Eu(III) chelates would be enhanced. There should be a gradient through the silica layer from the metal-silica surface to the external surface in which the Eu(III) chelates could emit luminescence with the intensity from quenching to

enhancement dependent on the distance. But the total intensity was observed to enhance due the near-field interactions. Both the quenching and enhancement for the Eu(III) chelates on the metal rods could be accompanied with a decrease of lifetime. In this study, we expected that the near-field interaction for the Eu(III) chelate on the silver rod could increase the radiative rate of Eu(III) chelate and furthermore increase the cyclic number for the excitation/emission of Eu(III) chelate in a period of time and increase the photon count rate in the measurement.

Polarized emission from a fluorophore is an important feature for its applications. But the lanthanides generally involve multiple transition dipole moments that are energetically degenerated during their emission. As a result, the emissions from the lanthanide dyes are a lack of polarization.[23] In addition, extremely long lifetimes of the lanthanides may bring up their free rotational motions in the excited states leading to loss of polarized emission. Some efforts have been done to initiate the polarized emission from the lanthanides but few progresses were achieved.[24,25] It is reported that the near-field interaction of a fluorophore with a metal nanoparticle can initiate a directional emission.[26a] In this study, we pursued to initiate a polarized emission from the Eu(III) chelates on the metal rods by the near-field interactions. The emission measurements were conducted in a single-channel method that was equipped with two orthogonal polarizations – one parallel and one perpendicular to the excitation polarization vector.[4] The emission intensities ($I_{\parallel}$ and $I_{\perp}$) have been normalized to correct for the polarization sensitivity of the detection pathway. The angle-dependent data were collected and presented in Figure 7. As expected, the metal-free Eu-contained silica templates displayed almost unpolarized emission (part a of Figure 7) because of their inherent characteristics, whereas the Eu–Ag rod complexes displayed a significant polarized emission (part b of Figure 7). As controls, the Eu–Au rod complexes and Eu–Ag sphere complexes were also determined under the same conditions. It was shown that the emission from the Eu–Au rod complexes was completely unpolarized but the emission from the Eu–Ag sphere complexes displayed a weak polarization. The emission anisotropies were calculated in eq 2. The value was 0.09 for the Eu–Ag rod complexes and 0.04 for the Eu–Ag sphere complexes. These values were lower in comparison with the anisotropies of most organic fluorophores in the solid substrates but acceptable in comparison with the anisotropies of the Eu(III) chelates in the aligned matrixes.[23–25] The polarized emission from the Eu–Ag rod complexes or Eu–Ag sphere complexes should arise from the near-field interactions. A stronger interaction on the silver rod might result in a larger decrease in the lifetime of the Eu(III) chelate, and thus the rotational motions of Eu(III) chelate on the silver rod should be severely restricted in a shorter excitation period. In addition, a stronger interaction of Eu(III) chelate with the silver rod might probably break up more efficiently the multiple transition dipole moments of Eu(III) chelate and become energetically undegenerated. Consequently, the emission from the Eu(III) chelate became polarized. We also notice that the emission from the Eu(III) chelate on the gold rod was completely unpolarized, which was primarily due to weak near-field interaction.

We consider that the plasmon resonance from the silver rods can extend to far field and contribute the polarized emission from the Eu–Ag rod complexes.[34,35] It is believed that when a fluorophores is coupled with a metal rod, the enhanced emission from the fluorophore–metal complex should have a component of plasmon energy by the metal nanoparticle extended to the far field at the same wavelength of fluorophore emission.[9,26a] The plasmon resonance from the metal nanoparticle is extended with the specific directions polarized,[35] so the fluorophore–metal complexes can emit the luminescence with the polarization. Relative to the silver spheres, the silver rods are considered to emit the plasmon resonances with more specifically directional property that may bring up more polarized emission.

SUMMARY

We studied the improved optical properties for the Eu(III) chelates on the metal nanorods due to the near-field interactions. The silver rods were fabricated in a wet chemical method followed by depositing thin silica layers on the surfaces. The Eu(III) chelates were followed by physically absorbing the silica layers on the silver rods. The silver rods displayed two plasmon bands, which had maxima close to the absorption and emission bands of the Eu(III) chelates. Thus, the Eu(III) chelates were expected to have strong interactions with the silver rods leading to greatly improved optical properties. The emission intensity could be enhanced up to 240-fold. Considering there were ca. 650 Eu(III) chelates on one silver rod, it was estimated that one Eu–Ag rod complex should be more than 1.5×10^5-fold brighter than one single free Eu(III) chelate. Because of the near-field interactions, the radiative rate of Eu(III) chelates on the silver rods is greatly increased leading to a dramatic decrease of lifetime from hundreds to several microseconds. However, this value is much longer than the lifetimes of most organic dyes, so the Eu–Ag rod complexes can be considered to use for time-resolved cellular assays. The gold rods or silver spheres were fabricated and conjugated with the Eu(III) chelates. The optical properties were measured as the controls of Eu–Ag rod complexes. It was found that both the gold rods and silver spheres had their plasmon bands only in part overlapping with the absorption and emission bands from the Eu(III) chelates leading to weaker near-field interactions. Consequently, the Eu–Au rod complexes and Eu–Ag sphere complexes had their optical properties less improved in comparison with the Eu–Ag rod complexes. It was also interesting to notice that the emission from the Eu(III) chelates on the silver rods was polarized, whereas the emission from others was almost not. This observation p supports that the sufficient near-field interactions for the fluorophores with the metal nanoparticles are essential for polarized initiation.

Acknowledgments

The authors would like to thank support by grants from NIH (EB009509, HG-002655, HG005090, EB006521, and CA134386).

REFERENCES

1. Binnemans K. Lanthanide-Based Luminescent Hybrid Materials. Chem. Rev. 2009; 109(4283): 4283–4374. [PubMed: 19650663] Bnzli J-CG. Lanthanide Luminescence for Biomedical Analyses and Imaging. Chem. Rev. 2010; 110:2729–2755. [PubMed: 20151630]
2. Moore EG, Samuel APS, Raymond KN. From Antenna to Assay: Lessons Learned in Lanthanide Luminescence. Acc. Chem. Res. 2009; 42:542–552. [PubMed: 19323456]
3. Sameiro M, Gonçalves T. Fluorescent Labeling of Biomolecules with Organic Probes. Chem. Rev. 2009; 109:190–212. [PubMed: 19105748]
4. Lakowicz, JR. Principles of Fluorescence Spectroscopy. 3rd ed. New York: Kluwer Academic/ Plenum Published; 2006.
5. Ma Y, Wang Y. Recent Advances in The Sensitized Luminescence of Organic Europium Complexes. Coord. Chem. Rev. 2010; 254:972–990.
6. Yu J, Parker D, Pal R, Poole RA, Cann MJ. A Europium Complex That Selectively Stains Nucleoli of Cells. J. Am. Chem. Soc. 2006; 128:2294–2299. [PubMed: 16478184]
7. Halas NJ, Lal S, Chang W-S, Link S, Nordlander P. Plasmons in Strongly Coupled Metallic Nanostructures. Chem. Rev. 2011; 111:3913–3961. [PubMed: 21542636]
8. Giannini V, Fernandez-Domínguez AI, Heck SC, Maier SA. SA Plasmonic Nanoantennas: Fundamentals and Their Use in Controlling the Radiative Properties of Nanoemitters. Chem. Rev. 2011; 111:3888–3912. [PubMed: 21434605]
9. (a) Lakowicz JR. Radiative Decay Engineering 5: Metal-Enhanced Fluorescence and Plasmon Emission. Anal. Biochem. 2005; 337:171. [PubMed: 15691498] (b) Lakowicz JR. Radiative Decay

Engineering: Biophysical and Biomedical Applications. Anal. Biochem. 2001; 298:1–24. [PubMed: 11673890]

10. (a) Sokolov K, Chumanov G, Cotton TM. Enhancement of Molecular Fluorescence Near the Surface of Colloidal Metal Films. Anal. Chem. 1998; 70:3898–3905. [PubMed: 9751028] (b) Ming T, Zhao L, Yang Z, Chen H, Sun L, Wang J, Yan C. Strong Polarization Dependence of Plasmon-Enhanced Fluorescence on Single Gold Nanorods. Nano Lett. 2009; 9:3896–3903. [PubMed: 19754068]
11. Morton SM, Silverstein DW, Jensen L. Heoretical Studies of Plasmonics Using Electronic Structure Methods. Chem. Rev. 2011; 111:3962–3994. [PubMed: 21344862]
12. (a) Eichelbaum M, Rademann K. Plasmonic Enhancement or Energy Transfer? On the Luminescence of Gold-, Silver-, and Lanthanide-Doped Silicate Glasses and Its Potential for Light-Emitting Devices. Adv. Funct. Mater. 2009; 19:2045–2052.(b) Nabika H, Deki S. Enhancing and Quenching Functions of Silver Nanoparticles on the Luminescent Properties of Europium Complex in the Solution Phase. J. Phys. Chem. B. 2003; 107:9161–9164.(c) Selvan ST, Hayakawa T, Nogami M. Remarkable Influence of Silver Islands on the Enhancement of Fluorescence from Eu3+ Ion-Doped Silica Gels. J. Phys. Chem. B. 1999; 103:7064–7067.(d) Malta OL, Santa-Cruz PA, De Sá GF, Auzel F. Fluorescence Enhancement Induced by the Presence of Small Silver Particles in Eu^{3+} Doped Materials. J. Lumin. 1985; 33:261–272.
13. Blair S, Lowe MP, Mathieu CE, Parker D, Senanayake PK, Kataky R. Narrow-Range Optical pH Sensors Based on Luminescent Europium and Terbium Complexes Immobilized in a Sol Gel Glass. Inorg. Chem. 2001; 40:5860–5867. [PubMed: 11681897] (b) Zhang J, Fu Y, Lakowicz JR. Luminescent Silica Core/Silver Shell Encapsulated with Eu (III) Complex. J. Phys. Chem. C. 2009; 113:19404–19410.
14. (a) Enderlein J. Spectral Properties of A Fluorescing Molecule within A Spherical Metallic Nanocavity. Phys. Chem. Chem. Phys. 2002; 4:2780–2786.(b) Enderlein J. Theoretical Study of Single Molecule Fluorescence in A Metallic Nanocavity. Appl. Phys. Lett. 2002; 80:315–317.
15. Zhang J, Fu Y, Chowdhury M, Lakowicz JR. Single-Molecule Studies on Fluorescently Labeled Silver Particles: Effects of Particle Size. J. Phys. Chem. C. 2008; 112:18–26.
16. Jain P, Huang K, El-Sayed X, El-Sayed IH, Noble MA. Metals on the Nanoscale: Optical and Photothermal Properties and Some Applications in Imaging, Sensing, Biology, and Medicine. Acc Chem. Res. 2008; 41:1578–1586. [PubMed: 18447366]
17. Rycenga M, Cobley CM, Zeng J, Li W, Moran CH, Zhang Q, Qin D, Xia Y. Controlling the Synthesis and Assembly of Silver Nanostructures for Plasmonic Applications. Chem. Rev. 2011; 111:36693712.
18. Schwartzberg AM, Zhang JZ. Novel Optical Properties and Emerging Applications of Metal Nanostructures. J. Phys. Chem. C. 2008; 112:10323–10337.
19. Fang X, Cao Z, Beck T, Tan W. Molecular Aptamer for Real-Time Oncoprotein Platelet-Derived Growth Factor Monitoring by Fluorescence Anisotropy. Anal. Chem. 2001; 73:5752–5257. [PubMed: 11774917]
20. Deprez E, Tauc P, Leh H, Mouscadet JF, Auclair C, Brochon JC. Oligomeric States of the HIV-1 Integrase as Measured by Time-Resolved Fluorescence Anisotropy. Biochemistry. 2000; 39:9275–9284. [PubMed: 10924120]
21. Eriksson O, Brooks MSS, Johansson B. Orbital Polarization in Narrow-Band Systems: Application to Volume Collapses in Light Lanthanides. Phys. Rev. B. 1990; 41:7311–7314.
22. Bunzli J-CG, Piguet C. Taking Advantage of Luminescent Lanthanide Ions. Chem. Soc. Rev. 2005; 34:1048–1077. [PubMed: 16284671]
23. (a) Seitz M, Moore EG, Ingram AJ, Muller G, Raymond KN. Enantiopure, Octadentate Ligands as Sensitizers for Europium and Terbium Circularly Polarized Luminescence in Aqueous Solution. J. Am. Chem. Soc. 2007; 129:15468–15470. [PubMed: 18031042] (b) Blanc J, Ross DL. Polarized Absorption and Emission in an Octacoordinate Chelate of Eu^{3+} . J. Chem. Phys. 1965; 43:1286–1289.
24. (a) Galyametdinov YG, Knyazev AA, Dzhabarov VI, Cardinaels T, Driesen K, Görller-Walrand C, Binnemans K. Polarized Luminescence from Aligned Samples of Nematogenic Lanthanide Complexes. Adv. Mater. 2008; 20:252–257.(b) Driesen K, Vaes C, Cardinaels T, Goossens K, Görller-Walrand C, Binnemans K. Polarized Luminescence of Non-mesogenic Europium-(III)

Complexes Doped into a Nematic Liquid Crystal. J. Phys. Chem. B. 2009; 113:10575–10579. [PubMed: 19601595]

25. (a) Hasegwa M, Ishii A, Furukawa K, Ohtsu H. Polarized ff-Emission of Terbium(III) by Using the Stretched Polymer Film Technique. J. Photopolym. Sci. Technor. 2008; 21:333–338.(b) Wu S, Yu X, Huang J, Shen J, Yan Q, Wang X, Wu W, Luo Y, Wang K, Zhang Q. Optically Controllable Polarized Luminescence from Azopolymer Films Doped with A Lanthanide Complex. J. Mater. Chem. 2008; 18:3223–3229.(c) Srdanov VI, Robinson MR, Bartl MH, Bu X, Bazan GC. Polarization Effects of A Europium Complex in Stretched Polyethylene. Appl. Phys. Lett. 2002; 80:3042–3044.(d) Yang CY, Srdanov V, Robinson MR, Bazan GC, Heeger AJ. Orienting $Eu(dnm)_3$ phen by Tensile Drawing in Polyethylene: Polarized Eu^{3+} Emission. Adv. Mater. 2002; 14:980–983.
26. (a) Lu L, Wang L-L, Zou C-L, Ren X-F, Dong C-H, Sun F-W, Yu S-H, Guo G-C. Doubly and Triply Coupled Nanowire Antennas. J. Phys. Chem. C. 2012; 116:23779–23784.(b) Murphy CJ, Sau TK, Gole AM, Orendorff, Cuo J, Gao J, Gou L, Hunyadi SE, Li T. Anisotropic Metal Nanoparticles: Synthesis, Assembly, and Optical Applications. J. Phys. Chem. B. 2005; 109:13857–13870. [PubMed: 16852739]
27. Jana NR, Gearheart L, Murphy CJ. Wet Chemical Synthesis of Silver Nanorods and Nanowires of Controllable Aspect Ratio. Chem. Commun. 2001:617–618.
28. Fu Y, Zhang J, Lakowicz JR. Plasmon-Enhanced Fluorescence from Single Fluorophores End-Linked to Gold Nanorods. J. Am. Chem. Soc. 2010; 132:5540–5541. [PubMed: 20364827]
29. Stöber W, Fink A, Bohn E. Controlled Growth of Monodisperse Silica Spheres in the Micron Size Range. J. Colloid Interface Sci. 1968; 26:62–69.
30. Zhang J, Gryczynski I, Gryczynski Z, Lakowicz JR. Dye-Labeled Silver Nanoshell-Bright Particle. J. Phys. Chem. B. 2006; 110:8986–8991. [PubMed: 16671705]
31. Hu J, Zhang J, Liu F, Kittredge F, Whitesell JK, Fox M. A Competitive Photochemical Reactivity in a Self-Assembled Monolayer on a Colloidal Gold Cluster. J. Am. Chem. Soc. 2001; 123:1464–1470.
32. Rosi NL, Mirkin CA. Nanostructures in Biodiagnostics. Chem. Rev. 2005; 105:1547–1562. [PubMed: 15826019]
33. Driesen K, VanDeun R, Gorller-Walrand C, Binnemans K. Near-Infrared Luminescence of Lanthanide Calcein and Lanthanide Dipicolinate Complexes Doped into A Silica-PEG Hybrid Material. Chem. Mater. 2004; 16:1531–1535.
34. Szmacinski H, Lakowicz JR. Depolarization of Surface-Enhanced Fluorescence: An Approach to Fluorescence Polarization. Assays. Anal. Chem. 2008; 80:6260–6266.
35. Motegi T, Nabika H, Niidome Y, Murakoshi K. Observation of Defocus Images of a Single Metal Nanorod. J. Phys. Chem. C. 2013; 117:2535–2540.

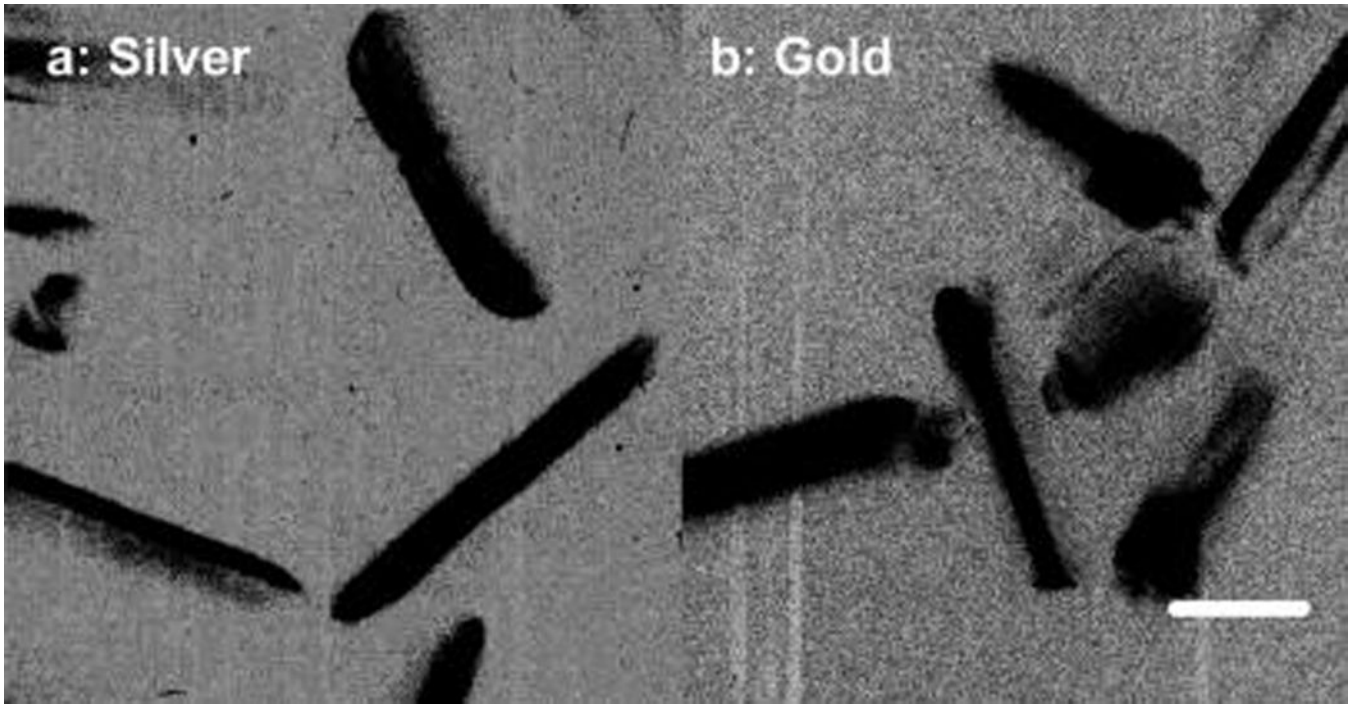

Figure 1.
Low-resolution TEM images of (a) silver and (b) gold nanorods. The scale bar in the image is 20 nm.

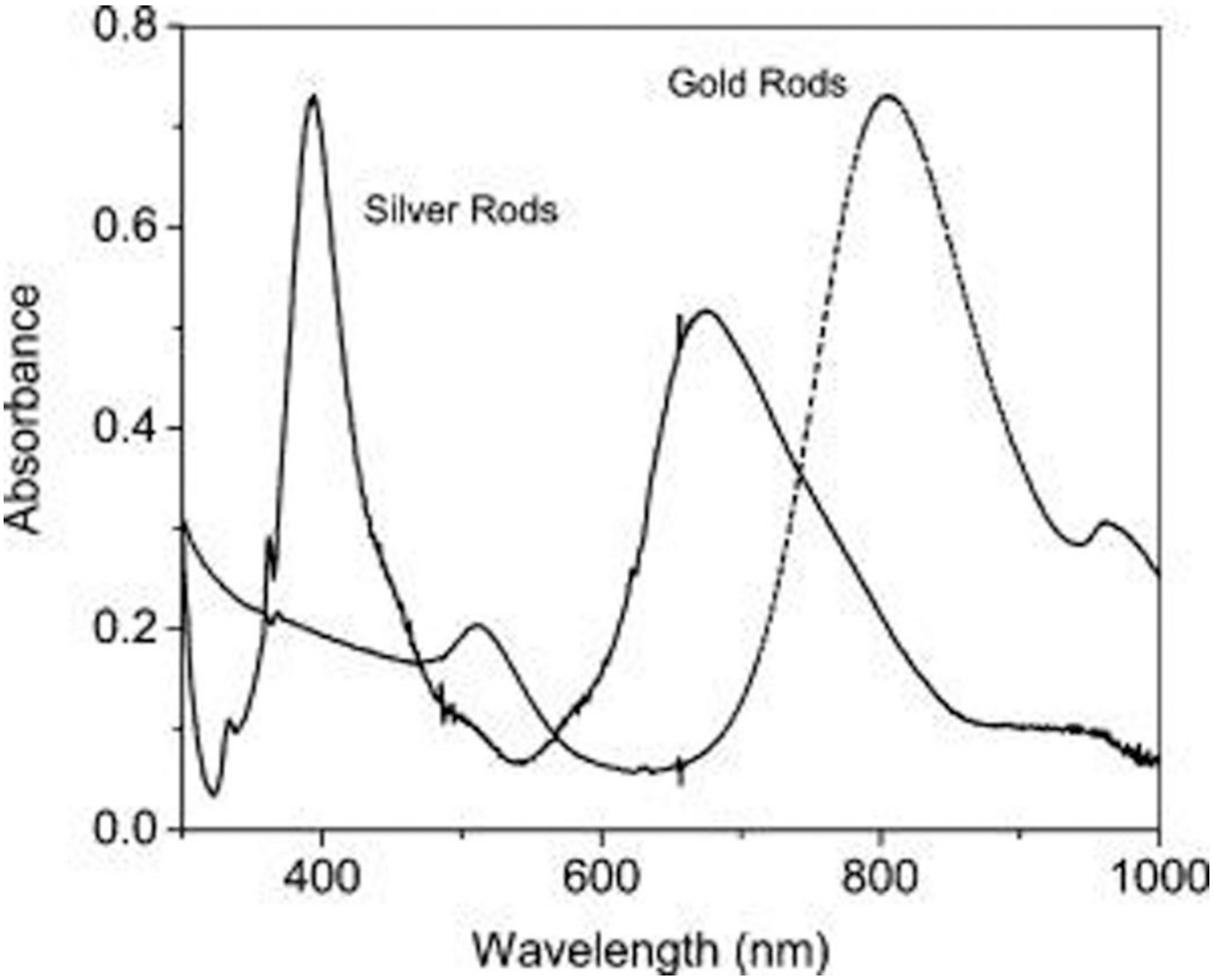

Figure 2.
Ensemble absorption spectra of silver and gold nanorods in aqueous solutions.

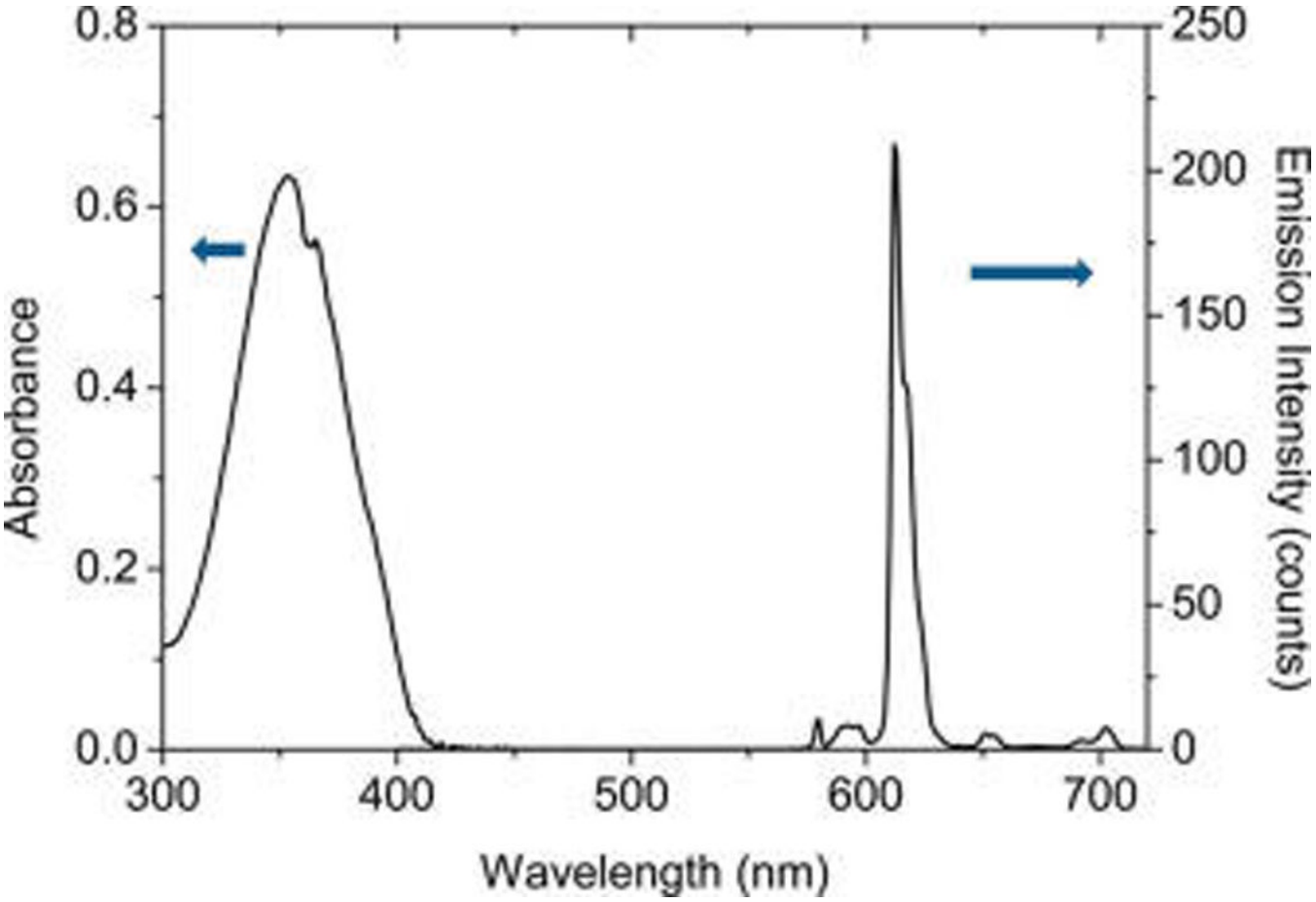

Figure 3.
Ensemble absorption and emission spectra of Eu(III) chelate in dimethylformamide (DMF) solution. The emission spectrum was collected upon excitation at 380 nm. The gate pulse width was controlled to be 0.5 ms and the delay time was 0.1 ms.

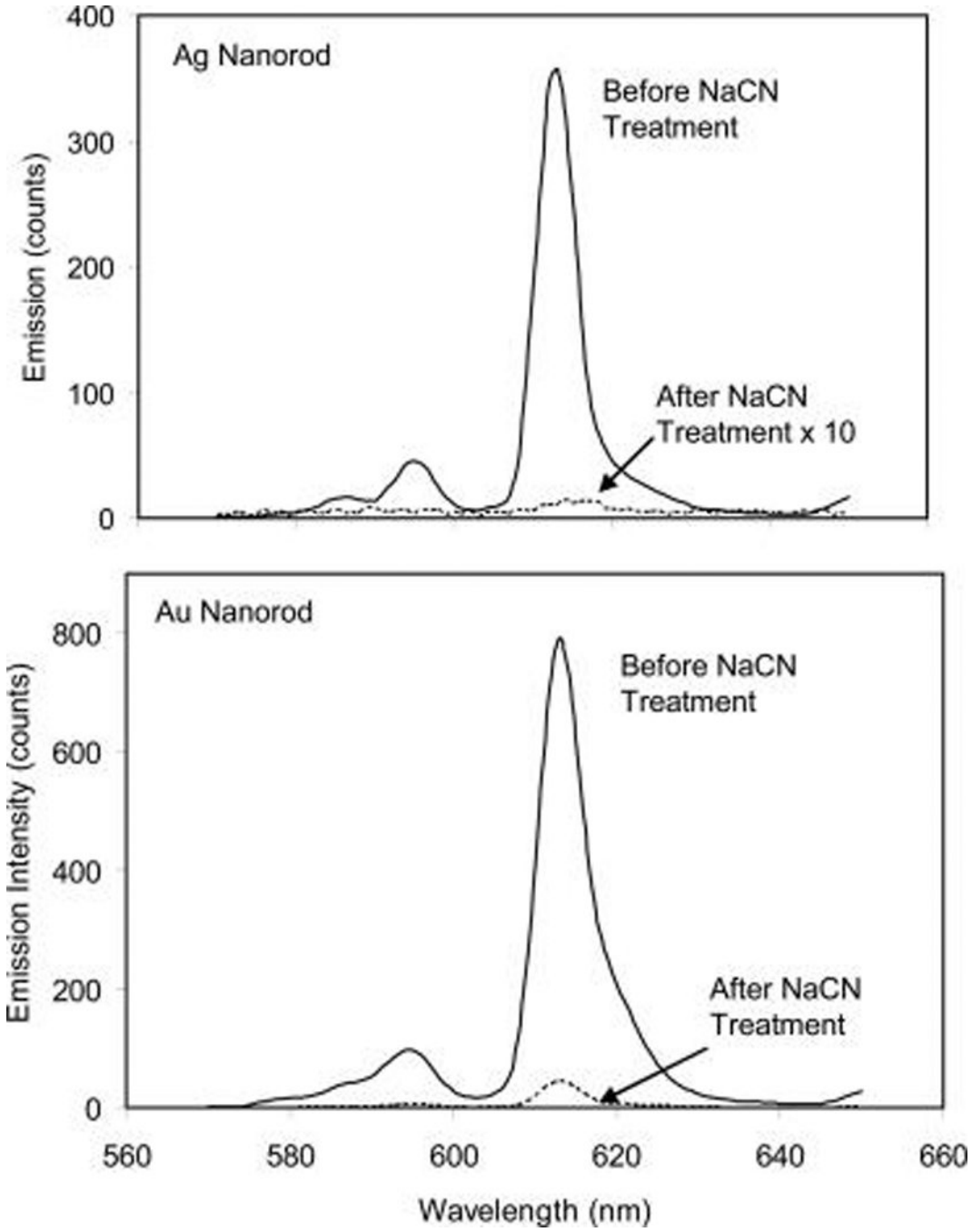

Figure 4.

Emission spectral changes for the Eu(III) chelates on the Ag rods and gold rods in aqueous solution prior to and after NaCN treatment. The emission spectra were collected upon excitation at 380 nm. The gate pulse width was controlled to be 0.5 ms and the delay time was 0.1 ms.

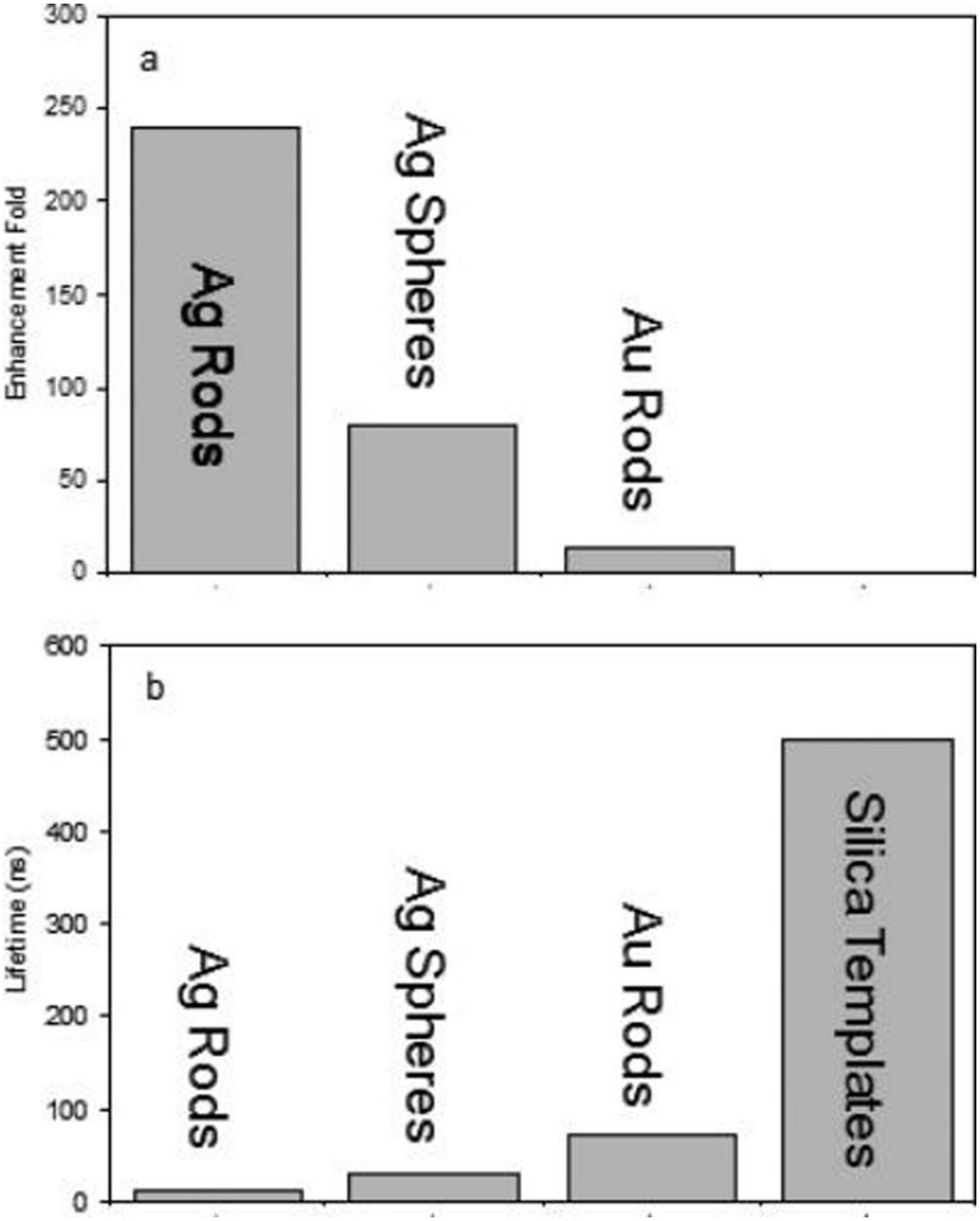

Figure 5.
(a) Enhancement folds of emission intensity for the Eu(III) chelates on the metal nanoparticles in comparison with the emission intensity for the Eu(III) chelate in the metal-free silica templates and (b) reduced lifetimes for the Eu(III) chelates on the metal nanoparticles.

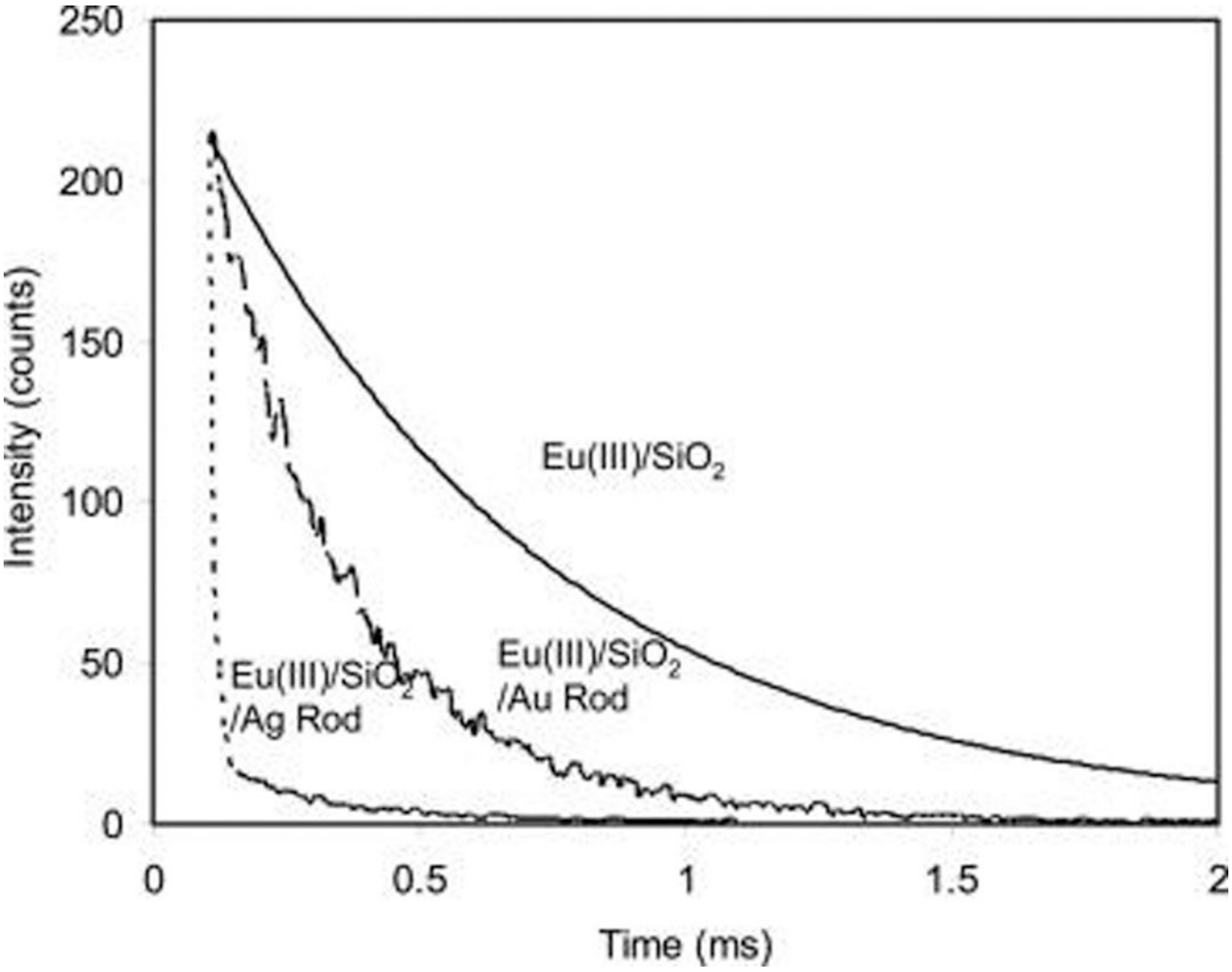

Figure 6.
Decay curves of Eu(III) chelates on the metal-free silica templates, silver rods, and gold rods. The decay curves were collected upon excitation at 380 nm. The gate pulse width was controlled to be 0.5 ms and the delay time was 0.1 ms.

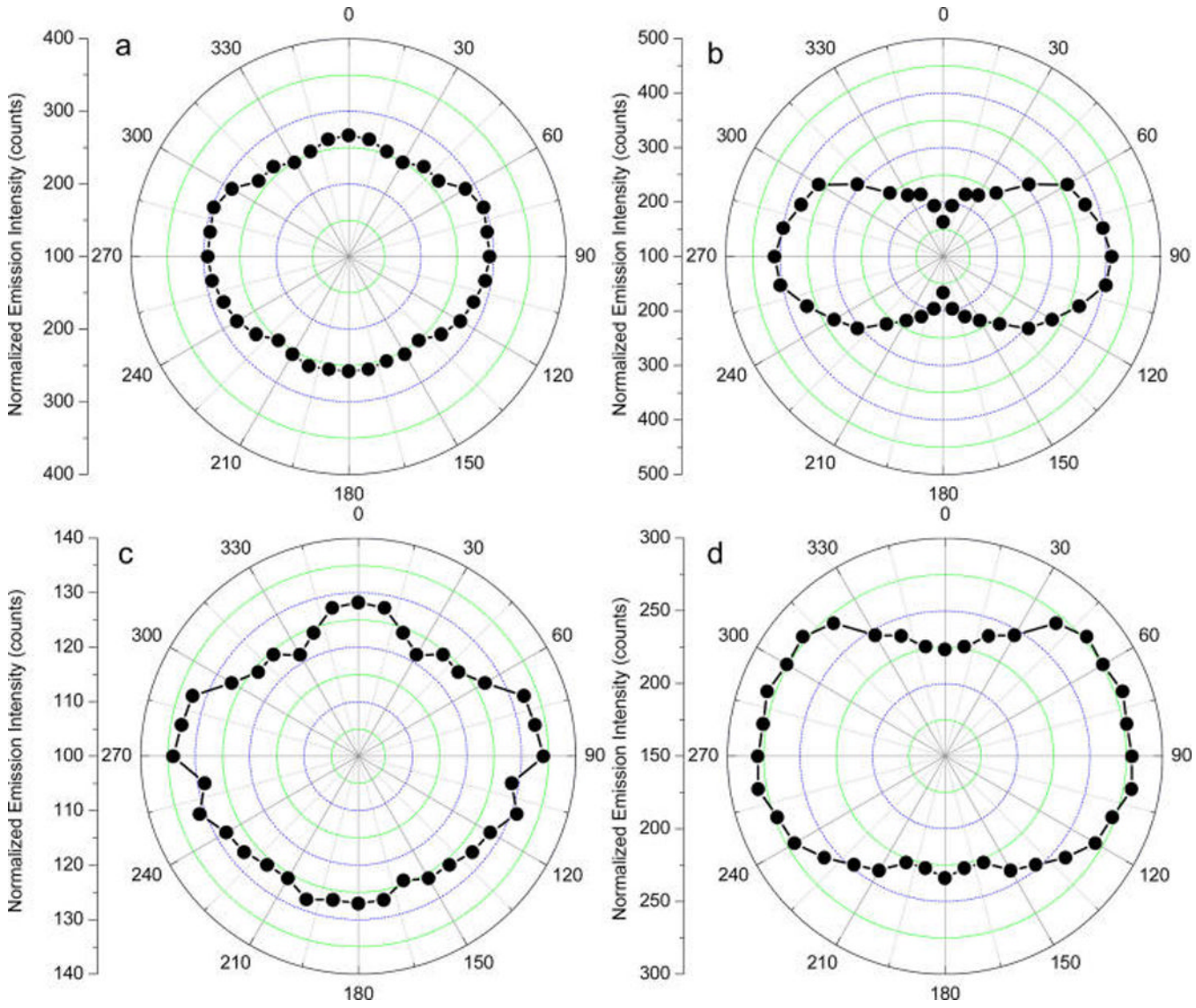

Figure 7.

Emission intensity as a function of excitation laser polarization for (a) Eu–silica templates, (b) Eu–Ag rod complexes, (c) Eu–Au rod complexes, and (d) Eu–Ag sphere complexes. The emission intensity at 614 nm was collected upon excitation at 380 nm. The gate pulse width was controlled to be 0.5 ms and the delay time was 0.1 ms.